TECHNICAL NOTES

NATIONAL ADVISORY COMMITTEE FOR AERONAUTICS

No. 915

THE EFFECT OF INLET-VALVE DESIGN, SIZE, AND LIFT ON THE AIR CAPACITY AND OUTPUT OF A FOUR-STROKE ENGINE

By James C. Livengood and John D. Stanitz
Massachusetts Institute of Technology

Washington
November 1943

NATIONAL ADVISORY COMMITTEE FOR AERONAUTICS

TECHNICAL NOTE NO. 915

THE EFFECT OF INLET-VALVE DESIGN, SIZE, AND LIFT ON THE AIR CAPACITY AND OUTPUT OF A FOUR-STROKE ENGINE

By James C. Livengood and John D. Stanitz

SUMMARY

A series of performance tests has been made with a CFR engine at constant inlet pressure and temperature and constant exhaust pressure. Special cylinder heads with different sizes and designs of inlet valve and port were used. The valves were tested at several lifts - both in the engine and in a steady-flow apparatus.

It was found that the variation of volumetric efficiency resulting from changes in valve design, size, and lift could be expressed as a function of

Mach No?

$$\frac{\text{piston speed} \times \text{piston area}}{\text{sound velocity} \times \text{valve area} \times \text{average flow coefficient}}$$

provided that other design ratios and operating conditions were kept constant. The average flow coefficient was determined from steady-flow tests of the valve and port and from the diagram of valve opening against crank angle. The valve area was the area of the valve head based upon the minimum diameter of contact between valve and seat. Sound velocity was computed for air at inlet-mixture temperature.

INTRODUCTION

The factors which affect the volumetric efficienty of an internal combustion engine may be classified into two categories:

(1) Operating conditions, such as revolutions per minute, inlet and exhaust pressures, operating temperatures, and so forth

(2) Design factors, including design of cylinder, valves, inlet and exhaust manifolds, valve timing, and so forth

This investigation was carried out to determine the effect of inlet-valve design, size, and lift on volumetric efficiency at several engine speeds. In order to accommodate valves of different sizes, the cylinder end of the inlet port had a different diameter for each size of valve tested. All other operating conditions and design ratios were held constant.

In references 1 and 2 reports were made of previous investigations at Massachusetts Institute of Technology on the relative importance of inertia of the air columns, fluid friction, and heat transfer upon volumetric efficiency. In these reports it was shown that, at low air velocities, the valve and port affect the volumetric efficiency chiefly by increasing the temperature of the charge in the cylinder. At higher velocities the volumetric efficiency may also be reduced by a lowering of the pressure in the cylinder at the time of inlet closing.

Methods have been developed for experimentally determining the resistance offered to steady air flow by different designs of port and valve. (See references 3, 4, 5, and 6.) The measure of this resistance is embodied in the curve of steady-flow coefficient against lift-diameter ratio obtained by static-flow tests. This type of testing is described in appendix A.

Resistance to flow can be reduced by the following means: (1) increasing the valve area; (2) increasing the valve lift; and (3) improving the valve and port design.

At the present time these facts are recognized by designers, but as yet no means have been developed by which it is possible to predict the quantitative effect that changes in these factors will have on the volumetric efficiency and power output of an engine. The purpose of this research was to investigate the possibility of such a prediction by correlating the curves of volumetric efficiency against piston speed of an engine operating with different sizes and designs of inlet valve and port and observing the corresponding trends in power output.

The objects of the tests were:

(1) To investigate the possibility of correlating the relationships between volumetric efficiency and piston speed of a given engine operated with inlet valves and ports of different size but of similar design

(2) To determine whether such a correlation can be applied when the engine is operated with a given inlet valve at several lifts

(3) To determine whether the correlation for the case of geometrically similar valves can be satisfactorily applied when dissimilar valves are used

(4) To determine whether, under the conditions of the tests, changes in volumetric efficiency produce corresponding changes in mean effective pressure

The tests were made at the Sloan Laboratories of the Massachusetts Institute of Technology with the financial assistance of the National Advisory Committee for Aeronautics.

DESCRIPTION OF APPARATUS

Engine

The engine used was a CFR single-cylinder, water-cooled engine of 3.25-inch bore and 4.5-inch stroke (figs. 1 and 2). The cylinder used was an old style with removable head. (A special steel flywheel was used, and a heavy-duty connecting rod with removable crankpin bearing shells was used after the usual babbitt type failed to stand up at high speeds.)

Four cylinder heads were used (fig. 3); they were identical with the exception of the inlet valves and seats and the lower portion of the inlet ports. A standard CFR exhaust valve was used. An aluminum spacer between the cylinder and the cylinder head provided openings for two spark plugs. The compression ratio was 4.92. Ignition was provided by a breaker operating at crankshaft speed.

Inlet System

Air supplied to the engine was passed successively through a standard sharp-edge orifice, a 50-gallon orifice box, a throttle valve, a heated vaporizing tank, and an intake pipe leading to the engine. (See fig. 4.)

Inasmuch as the inlet pressure used for calculating volumetric efficiency was measured in the vaporizing tank, it was desirable to have negligible pressure drop through the intake pipe and freedom from resonance effects that would complicate an analysis of the results. Therefore, the intake pipe was made as short as practicable and was extremely large for the air flow through it. (See fig. 5.) An attempt to measure pressure waves in the inlet pipe demonstrated that the pressure variations were less than 5 percent of the mean absolute pressure.

Fuel and Fuel System

The fuel used was 73-octane aviation gasoline, both leaded and unleaded. The only critical characteristic was volatility, since no detonation was encountered even when 65-octane fuel was tried.

The gasoline was supplied by a pump to a steam-jacketed nozzle, where it was heated just prior to injection into the air stream entering the jacketed vaporizing tank. (See fig. 4.) With the tank walls heated sufficiently to maintain 120° F mixture temperature entering the engine, there was no trouble from condensation of aviation gasoline.

Exhaust System

The exhaust port was connected by a short pipe to a 5-gallon water-jacketed surge tank. The exhaust gases then passed through a throttle valve into the laboratory exhaust system. (See figs. 4 and 5.)

Cooling System

Cooling was provided by circulating water through the jackets by a separately driven pump. Jacket temperature was controlled by bleeding cold water or steam into the system as occasion required.

Lubrication

A separately driven gear pump forced lubricating oil into the oil gallery of the engine under pressure. The relatively large amount of oil bypassed by a relief valve was circulated through heat exchangers and returned to the sump in the engine base. This arrangement provided close control both of the temperature of the oil in the sump and that of the oil entering the oil gallery.

Valves

Stroboscopic observation of the operation of the standard Waukesha high-speed camshaft and special valve gear indicated that the valves ceased to follow the cam above 3800 rpm and bounced on closing at slightly higher speeds. Consequently a special high-speed cam and upper valve gear were designed. This mechanism provided extreme rigidity and enabled operation above 4400 rpm with no evidence of bouncing or failure to follow the cam. (See figs. 6 and 7.) An adjustable inlet rocker arm was the means of changing the lift.

Three of the inlet valves and ports used were of the same design (A, figs. 3 and 8). The elbows in the ports of all valves were of identical dimensions and were sufficiently large to offer small restriction to flow compared with the valve and seat. Below the elbow, the port was tapered to suit the particular valve for which it was intended. (See fig. 3.)

The diameters of the geometrically similar valves were arranged to give equal increments of area. All design ratios, as well as the calculation of the flow coefficients, were based on the minimum diameter of contact between valve and seat, D_2 in figure 8. Even the largest inlet valve was considerably smaller than the exhaust valve. The large exhaust valve was considered desirable in order to minimize variations due to exhaust effects.

The fourth inlet valve was of the same diameter as the largest valve of the geometrically similar series just described but was of different design (design B, figs. 3 and 8).

The three valves of design A, together with their ports, had identical curves of flow coefficient against lift-diameter ratio; the valve of design B had different flow characteristics. (See fig. 9.) In order to determine the flow-coefficient curve of the valve under steady-flow conditions, the valve and the cylinder were mounted as shown in figure 10. The air passed through the orifice box and into the valve port through a rounded approach. The valve lift was adjusted by a micrometer screw at the top of the cylinder. A constant pressure drop of 10 inches of alcohol was maintained across the valve by exhausting the cylinder with a vacuum pump. The method of computing the flow coefficient is described in appendix A.

Measuring Instruments

Torque was measured with a small electric cradle dynamometer and beam scales. Speed was determined by a mechanical tachometer in conjunction with a strobotac operating from a 60-cycle alternating-current line and illuminating 36 painted stripes on the flywheel.

Air flow was measured by a sharp-edge orifice and an NACA micromanometer. The orifice was constructed in accordance with the specifications given in reference 7.

All temperatures were measured with mercury-in-glass thermometers with the exception of oil temperatures, which were measured with vapor-pressure thermometers.

Fuel flow was measured by a rotameter, the calibration of which was frequently checked by a combination of weighing scales and an automatic stop clock.

Atmospheric pressure was measured with a mercury barometer, inlet pressure was measured in the vaporizing tank with a mercury manometer, and exhaust pressure was measured in the exhaust surge tank by the same means.

Valve lift was determined in the following manner: with the engine cold, the inlet-valve clearance was set to the hot value and the rocker-arm ratio was adjusted (fig. 6) until the desired lift was obtained when measured with a dial gage.

Spark advance was measured by a neon light (excited by the spark discharge), which revolved with the crankshaft adjacent to a stationary protractor.

PROCEDURE

The principal measurement required for these tests was the air capacity of the engine over a range of operating speeds. In order to make this measurement under comparative conditions, all variables were carefully controlled. This precaution made possible the calculation of other quantities that were an aid in discovering inconsistencies in the data and in determining the causes for any nonreproducibility of results.

Specifically, the following quantities were held constant at the values indicated:

Inlet-mixture temperature, °F	120
Vaporizing-tank pressure, inches of mercury absolute	27.4
Fuel-air ratio	0.078
Oil temperatures, °F	160
Jacket-water outlet temperature, °F	180
Exhaust surge-tank pressure, inches of mercury absolute	31.4
Inlet-valve and exhaust-valve running clearances, inch	0.010
Valve timing: Inlet opens, degrees B.T.C.	28
Valve timing: Inlet closes, degrees A.B.C.	58
Valve timing: Exhaust closes, degrees A.T.C.	28
Valve timing: Exhaust opens, degrees B.B.C.	58

The following quantities were varied:

(1) Engine speed

(2) Inlet-valve and lower port diameter

(3) Inlet-valve lift

(4) Inlet-valve design

(5) Spark advance (always for best power)

Several facts that affected the procedure were discovered.

(1) The curve of power output against fuel-air ratio was very flat for a considerable range of fuel-air ratios, and the best power fuel-air ratio did not change with speed. This result made it possible to use a constant value for fuel-air ratio instead of having to determine a new value for each set of conditions.

(2) The curve of power output against spark advance was very flat in all instances. This result made it difficult to determine the best power setting but, at the same time, reduced the error resulting from a mistake in judgment.

(3) Carbon deposits around the inlet valve remarkably increased resistance to flow through the valve and produced a corresponding reduction in air flow and power. This result made it necessary to remove the cylinder head for cleaning after each series of firing runs and to shorten the duration of each series as much as compatible with accuracy and reproducibility of results. Trouble from this cause was eliminated by taking these precautions.

TESTS

Each of the three similar inlet valves (design A) was operated at three lifts. Inlet valve B was operated at one lift. In each case the engine was run, both firing and motoring, over a speed range from 2000 to 4400 rpm, in 400 rpm increments. In addition to this principal set of runs, a preliminary set of runs was made to determine the proper fuel-air ratio and the sensitivity of output to spark advance.

The running time required for equilibrium conditions to be attained was shortened by circulating heated lubricating oil through the lubrication system and by circulating hot water through the jackets for approximately an hour before starting the engine. After the engine was started an additional one-half to three-quarters of an hour was required before complete temperature equilibrium was obtained. The air capacity seldom changed after 5 minutes of operation under a given set of conditions.

The speed was progressively increased from 2000 to 4400 rpm, and check points were taken before the engine was stopped. Several times during the course of these tests complete curves were rerun to check reproducibility of results, which was found to be unusually good.

RESULTS

The primary results of the tests are incorporated in figure 11, air capacity against piston speed; figure 12, brake horsepower against piston speed; and figure 13, motoring friction horsepower against piston speed. Subsequent curves are derived from these.

DISCUSSION OF RESULTS AND CORRELATION

Figure 11 shows a wide variation in air flow with both valve size and lift, especially at high piston speeds. Each of the curves seems to approach a limiting value of air flow at high speed. The reasonableness of this result can be seen by considering that the maximum possible air flow would be attained by having sonic velocity through the valve at all times. A calculation of this limit for the 0.950-inch-diameter valve operating at 0.238-inch lift gives a result of 0.035 pound of air per second; the engine test showed the maximum flow to be 0.0268 pound per second. The lift curve and the fact that the valve was off its seat only 226/720 the time (see cam-lift curve, fig. 7) was taken into account in this calculation, but no attempt was made to allow for temperature rise due to heat transferred to the air by the valve and port.

Of more interest for this report is the volumetric efficiency e, defined as follows:

$$e = \frac{M\ 60}{\frac{N}{2}\ \rho_i\ V_D}$$

where

M air capacity, pounds per second

N engine speed, revolutions per minute

ρ_i inlet density, pounds per cubic foot

V_D piston displacement, cubic feet

It has been shown by dimensional analysis (reference 8, p. 237 f.) that volumetric efficiency e can be expressed as a function of several variables. Neglecting heat transfer, the following quantities are believed to affect e:

SYMBOLS

ρ	air density at intake $(F\ L^{-4}\ T^{2})$
μ	air viscosity at intake $(F\ L^{-2}\ T)$
c	sound velocity in intake air $(L\ T^{-1})$
l	characteristic length of engine (L)
N	rotational speed of engine (T^{-1})
R_1, R_2, R_3, etc.	design ratios of engine and inlet system (0)

If these are all of the quantities affecting e, there may be written

$$e = \phi_1\,(\rho,\ \mu,\ c,\ l,\ N,\ R_1,\ R_2,\ R_3,\ \text{etc.})$$

and, by arranging them into nondimensional parameters,

$$e = \phi_2\left(\frac{\rho l^2 N}{\mu},\ \frac{lN}{c},\ R_1,\ R_2,\ R_3,\ \text{etc.}\right)$$

But lN is proportional to s, the piston speed, and $\frac{\rho l^2 N}{\mu}$ = constant × Re, where Re is the Reynolds number. Since the flow in most actual engines is well up in the turbulent region, it is reasonable to take no account of changes in the parameter $\frac{\rho l^2 N}{\mu}$. Hence

$$e = \phi_3 \left(\frac{s}{c}, R_1, R_2, R_3, \text{etc.}\right)$$

For geometrically similar engines with similar inlet systems R_1, R_2, R_3, and so forth, are constants, and

$$e = \phi_4 \left(\frac{s}{c}\right)$$

For the case of engines of different design, it is convenient to retain the parameter s/c and to modify the expression by introducing the design ratio

$$R_1 = \frac{\text{piston area}}{\text{valve area}}$$

and

$$R_2 = \frac{1}{\text{average flow coefficient}}$$

The reason for using the first of these design ratios is immediately seen to be an attempt to change piston speed s into the corresponding gas velocity through the inlet valve.

The average flow coefficient is defined in appendix B. It is based on the lift-against-crank angle curve, obtained from the cam-lift curve (fig. 7) and the rocker-arm ratio, and on the steady-flow coefficient obtained at each value of the lift. The introduction of the average flow coefficient as an additional design factor corrects the nominal valve area for the changing lift during the suction stroke, and also includes contraction effects through the "orifice" formed by the valve and seat. (See appendix A.)

In a normal engine, another important parameter is the ratio of intake-pipe length to stroke. In this case the effect of this parameter was purposely minimized by using a short pipe of large diameter, and it could therefore be ignored.

It might be expected that, for all engines with the same valve timing and with the same inlet and exhaust conditions, there would be a unique function,

$$e = \phi_5 \left(\frac{s}{c}, \frac{A_p}{A_v}, \frac{1}{C_{av}}\right)$$

where

s piston speed

c velocity of sound

A_p piston area

A_v nominal valve area

C_{av} average flow coefficient of valve (appendix B)

This equation will not, in general, hold if there are resonance effects in the inlet or exhaust systems, or if the heat transfer to a unit weight of charge during its passage into the cylinder varies appreciably with the valve size or design.

In order to test the above analysis, the volumetric efficiencies as determined from figure 10 were first plotted against

$$\frac{\text{piston speed} \times \text{piston area}}{\text{sound velocity} \times \text{valve area}}$$

as in figure 14. Valve area is $\frac{\pi D_2^2}{4}$ (fig. 8), and sound velocity is computed for air at inlet-mixture temperature. The most interesting point to note about the curves of figure 14 is that the three curves obtained with similar valves running at the same L_{max}/D_2 ratio (0.25) are practically identical over most of the speed range covered.

The correlation obtained by multiplying the abscissa scale of figure 14 by $\frac{0.445}{\text{average steady-flow coefficient}}$ is shown in figure 15. The factor 0.445 is the value of the average flow coefficient for valves of design A operating at $L_{max}/D_2 = 0.25$.

The correlation obtained by this method seems remarkably good. It may be noted that the curve for the valve of design B tends to show a slight departure in trend from the average of the points for the geometrically similar valves. This difference, together with the smaller departure of the other points from exact correlation, may be explained in part by the discussion which follows.

Thermal Effects

Forbes and Taylor (reference 2) have analyzed the temperature rise of the fresh charge entering an engine cylinder. For this purpose they divided the total temperature rise into three parts: heat transfer from valve and port to the flowing charge; pressure drop due to resistance to flow in the valve (with subsequent recompression and temp. rise); and, finally, the unaccounted-for temperature rise, a part of which was due to heat transferred to the stagnant charge from valve and port during the period while the valve was closed.

Several interesting facts resulted from this analysis. First, the computed temperature rise due to heat transfer to the flowing charge was slightly less at 1500 rpm than at 1000 rpm but was a much higher percentage of the total. Second, the temperature rise due to flow resistance doubled from 1000 to 1500 rpm, and the percentage of total temperature rise attributable to flow resistance trebled. Finally, the unaccounted-for temperature rise dropped from 56 to 26 percent as the speed was increased.

It now seems likely that this large change in the unaccounted-for temperature rise was at least partly due to a valve-timing peculiarity. The combination of late inlet-valve closing, slow speed, and large inlet valve probably caused some "blow-back" of charge into the inlet port before the valve closed, with the result that some portion of the charge passed three times through the valve instead of once; this action violates one of the assumptions used in calculating the heat transfer from the valve to the flowing charge.

The dimensional analysis in the present report takes no deliberate account of these important thermal effects, but it is likely that the average flow coefficient parameter does include a partial correction for heat transfer as long as the design of the valve is unchanged. Two similar valves operated at the same value of

$$\frac{\text{piston speed}}{\text{sound velocity}} \times \frac{\text{piston area}}{\text{valve area}} \times \frac{\text{a constant}}{\text{average flow coefficient}}$$

would be expected to transfer about the same amount of heat per pound of air passing through them, since the velocity over the surfaces is the same in the two instances. A possible difference would be due to variation in Reynolds number, which will probably have a very small effect over the range of sizes investigated.

On the other hand, it is not difficult to imagine that an improvement of flow by the addition, say, of straightening vanes in a port elbow might decrease the measured resistance to flow; but, in an engine, the increase in heat transfer resulting from increased surface area might cancel the gain due to improvement in measured flow coefficient.

It is not surprising, therefore, to find that the curves of figure 15 show better correlation between valves of the same design than with the valve of different design. This fact would seem to indicate that the additional parameters which must be introduced into the dimensional analysis to take care of heat transfer completely will be primarily functions of design.

Effects on Engine Power

It will be noted in figure 12 that maximum power output decreases and that the peaks of the curves occur at progressively lower piston speeds, as the inlet-valve diameter or lift is decreased. This effect is similar to the effect noticed when an engine is throttled in the ordinary manner. If it is assumed that indicated horsepower is proportional to air capacity (fig. 16 is a measure of the validity of this assumption), then it can be seen from the curves of figures 12 and 13 that the brake-horsepower curves will have the characteristics noted.

The peak brake horsepower occurs at the piston speed where friction horsepower is rising as rapidly as indicated horsepower.

The indicated horsepower may be expressed:

$$\text{ihp} = M\ F\ E_c\ \eta\ \frac{778}{550}$$

where

M air capacity, pounds per second

F fuel-air ratio

E_c heating value of the fuel, Btu per pound

η indicated thermal efficiency

The slope of the curve in figure 16 is proportional to the thermal efficiency η and the scatter of points gives an indication of how nearly constant the efficiency remained. Too much importance should not be attached to individual points in figure 15, because each point contains at least two appreciable errors. The first is the experimental error in measuring both the brake and friction horsepowers. The second is due to the assumption that the motoring friction is the same as the firing friction, which is not necessarily true (reference 8, p. 199).

CONCLUSIONS

1. Under the conditions of these tests the steady-state flow coefficient of the inlet valve and port was a useful measure of the actual coefficient under running conditions.

2. The variation of volumetric efficiency resulting from changes in valve design, size, and lift can be expressed as a function of piston speed, sound velocity, piston area, valve area, and average flow coefficient, provided that other design ratios and operating conditions are kept constant.

3. With the valve timing used, and over the speed range investigated, increasing either the inlet-valve diameter or lift improved volumetric efficiency and power output.

4. At values of lift-diameter ratio less than about 0.25, changing the inlet-valve lift had the same effect as changing the diameter, while for values about 0.25 the diameter had a greater effect than lift.

RECOMMENDATIONS

Attention is invited to the fact that nominal gas velocities through the inlet valve,

$$\frac{\text{piston speed} \times \text{piston area}}{\text{valve area}}$$

for these tests varied from 240 to 830 feet per second. In current aircraft engines at rated speed, this factor is in the neighborhood of 180 feet per second. This fact would indicate the desirability of extending this investigation through a lower range of nominal gas velocities.

Since variations in inlet-valve timing might have an important effect on inlet-valve performance, particularly in the lower speed range, it is recommended that any further work in this field include inlet-valve timing as a variable.

Massachusetts Institute of Technology,
Cambridge, Mass., April 1943.

APPENDIX A

METHODS OF DETERMINING FLOW COEFFICIENTS FOR STEADY FLOW

The Flow Coefficient

The steady-flow coefficient for poppet valves has been developed to serve as a basis upon which to compare various valve and port combinations (references 3, 4, 5, and 6). The flow coefficient is an inverse measure of the resistance to flow through the valve and port at a given lift.

In the determination of the flow coefficient, a constant pressure drop is created across the valve and the rate of mass flow is measured. For the low pressure drop usually used (10 in. alcohol), the flow coefficient is determined from the equation:

$$M = A_v \ C \sqrt{2 \ \rho \Delta p}$$

in which the flow coefficient C is the only unknown.

The flow coefficient is based upon the nominal valve area $\frac{\pi D_2^2}{4}$. Changes in the actual area of the valve opening as the valve is lifted are reflected in the flow coefficient.

In order to make possible the comparison of valves of different diameter, it is necessary to compare the flow coefficients on the basis of a nondimensional parameter, in this case L/D_2. In the steady-flow tests made for the present report a series of lifts was selected for each valve such that the flow coefficient was determined at intervals of 0.05 L/D from 0 to 0.35. Figure 9 shows the results of tests on the valves used in this investigation, and figure 10 shows the apparatus used.

The selection of the diameter upon which the valve area and the L/D ratio are based is optional. When different valves are compared, however, it is necessary to use the same characteristic diameter.

The flow coefficient of the valve at a given L/D is calculated from the measurements made with the previously described apparatus by the following convenient formula, developed in reference 6, by equating the air flow through the metering orifice to the air flow through the valve:

$$M = A_o\ C_o \sqrt{2\rho_1\ \Delta p_1} = A_v\ C \sqrt{2\rho_2\ \Delta p_2}$$

and

$$C = \frac{A_o\ C_o}{A_v} \sqrt{\frac{\Delta p_1}{\Delta p_2}}$$

provided that $\rho_1 \cong \rho_2$, which is equivalent to having

$$\Delta p_1 << p_1$$

where

M air flow, weight per unit time

C steady-flow coefficient of valve

C_o coefficient of metering orifice

A_v nominal valve area

A_o orifice area

Δp_1 pressure drop across orifice

Δp_2 pressure drop across valve

ρ_1 density at orifice

ρ_2 density at valve

Intermittent Flow

The curve of C against L/D calculated by the method just described is obtained under steady-flow conditions. In the internal-combustion engine the flow is intermittent. The application of steady-flow results to intermittent conditions was at first questioned (reference 3), but the validity of its use was later established by Waldron (reference 5). Waldron's tests, however, were run at speeds appreciably lower than those employed in the present tests. The validity of the application of the steady-flow coefficients to intermittent conditions at the highest crank speeds used here has not been established. The success of the correlation of the engine test data indicates, however, that the steady-flow coefficient is very useful, whether or not it is an accurate measure of the coefficient in actual intermittent flow.

APPENDIX B

THE AVERAGE FLOW COEFFICIENT

The average flow coefficient used in the correlation of data in figure 12 is defined as:

$$c_{av} = \frac{1}{\theta_o}\int_o^{\theta_o} C\, d\,\theta$$

where θ_o is the number of crank degrees during which the valve is open and C is the flow coefficient corresponding to a given crank angle.

The average flow coefficient was determined in the following manner: First, the valve-lift curve was obtained from the cam profile (fig. 7) and the rocker-arm ratio. From the curve of flow coefficient against lift-diameter ratio (fig. 9) it was then possible to plot a curve of C against θ (fig. 17).

The area under this curve was then measured with a planimeter, and the average flow coefficient C_{av} was obtained by dividing this area by the length of the abscissa θ_o and multiplying by a scale factor. The variation of C_{av} with L_{max}/D_2 is shown in figure 18.

REFERENCES

1. Reynolds, Blake, Schecter, Harry, and Taylor, E. S.: The Charging Process in a High-Speed, Single-Cylinder, Four-Stroke Engine. T.N. No. 675, NACA, 1939.

2. Forbes, J. E., and Taylor, E. S.: Rise in Temperature of the Charge in its Passage through the Inlet Valve and Port of an Air-Cooled Aircraft Engine Cylinder. T.N. No. 839, NACA, 1942.

3. Nutting, E. M., and Lewis, G. W.: Air Flow through Poppet Valves. Rep. No. 24, NACA, 1918.

4. Tanaka, Keikita: Air Flow through Suction Valve of Conical Seat. Rep. No. 50 (vol. IV, 9), Aero. Res. Inst., Tokyo Imperial Univ., Oct. 1929.

5. Waldron, C. D.: Intermittent-Flow Coefficients of a Poppet Valve. T.N. No. 701, NACA, 1939.

6. Wood, G. B., Jr., Hunter, D. U., Taylor, E. S., and Taylor, C. F.: Air Flow through Intake Valves. SAE Jour., vol. 50, no. 6, June 1942, pp. 212-220, 252.

7. Anon.: History of Orifice Meters and the Calibration, Construction, and Operation of Orifices for Metering. Report of the Joint A.G.A.-A.S.M.E. Committee on Orifice Coefficients. A.S.M.E., 1935, p. 30.

8. Taylor, C. Fayette, and Taylor, Edward S.: The Internal Combustion Engine. International Textbook Co. (Scranton, Pa.), 1938.

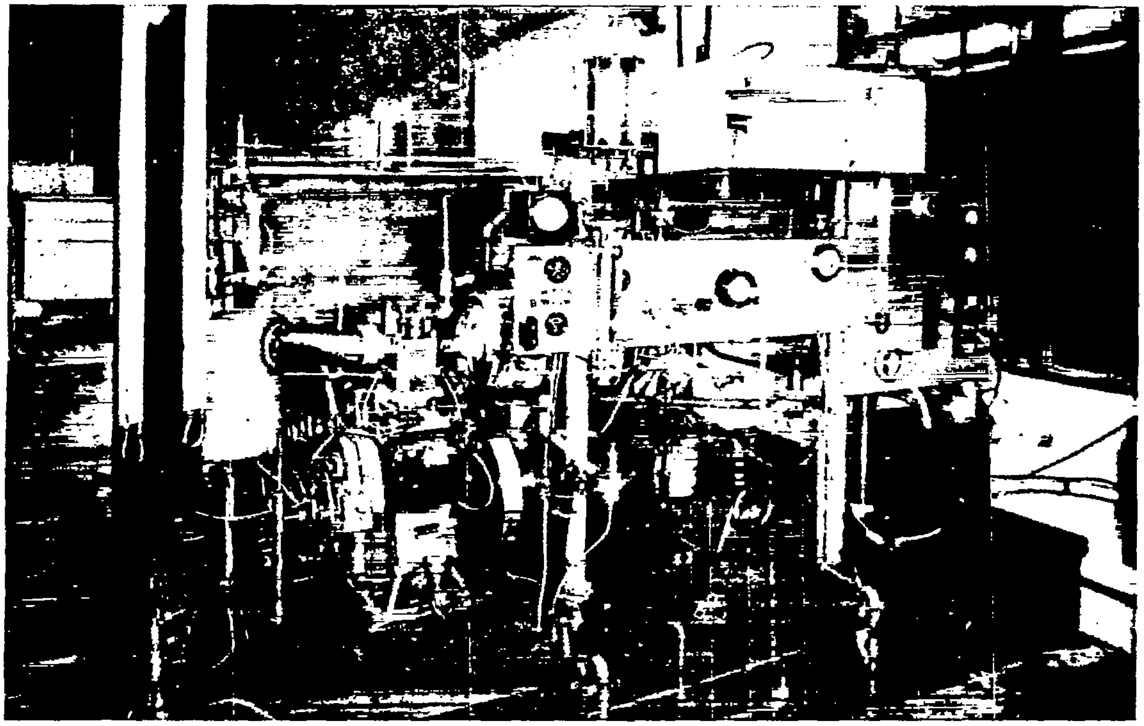

Figure 1.- General view of the apparatus showing engine, dynamometer and controls.

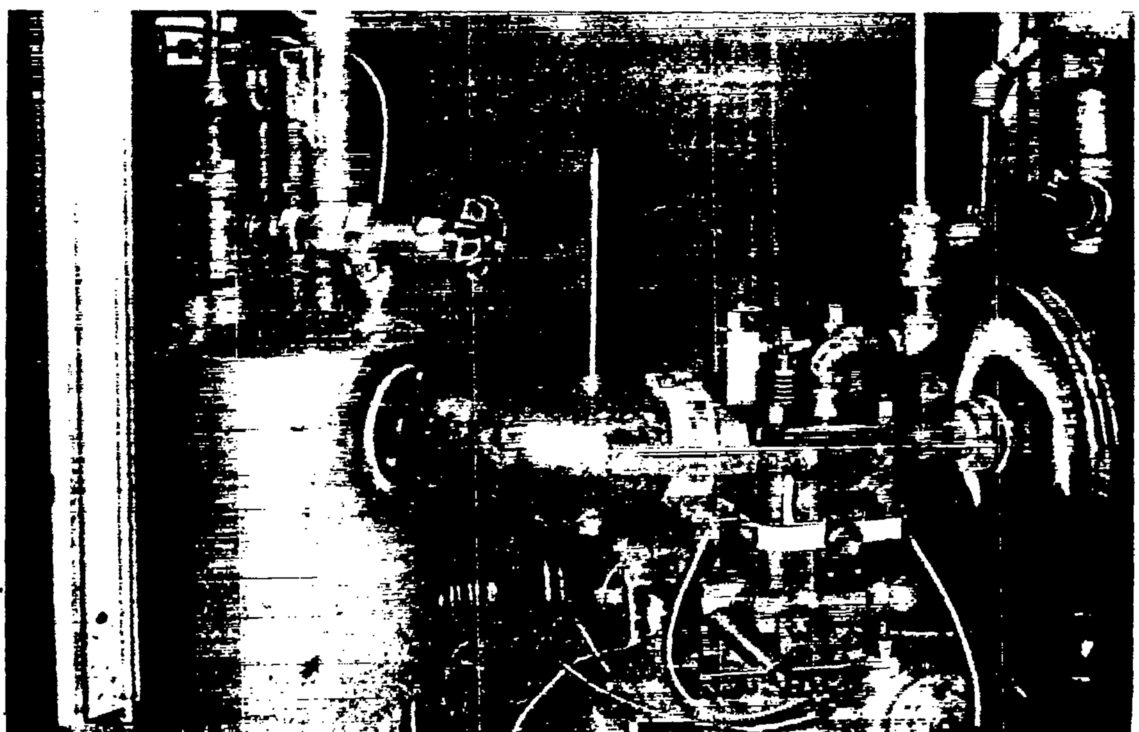

Figure 2.- Close-up of engine showing large intake pipe, adjustable inlet-valve rocker arm and short exhaust pipe

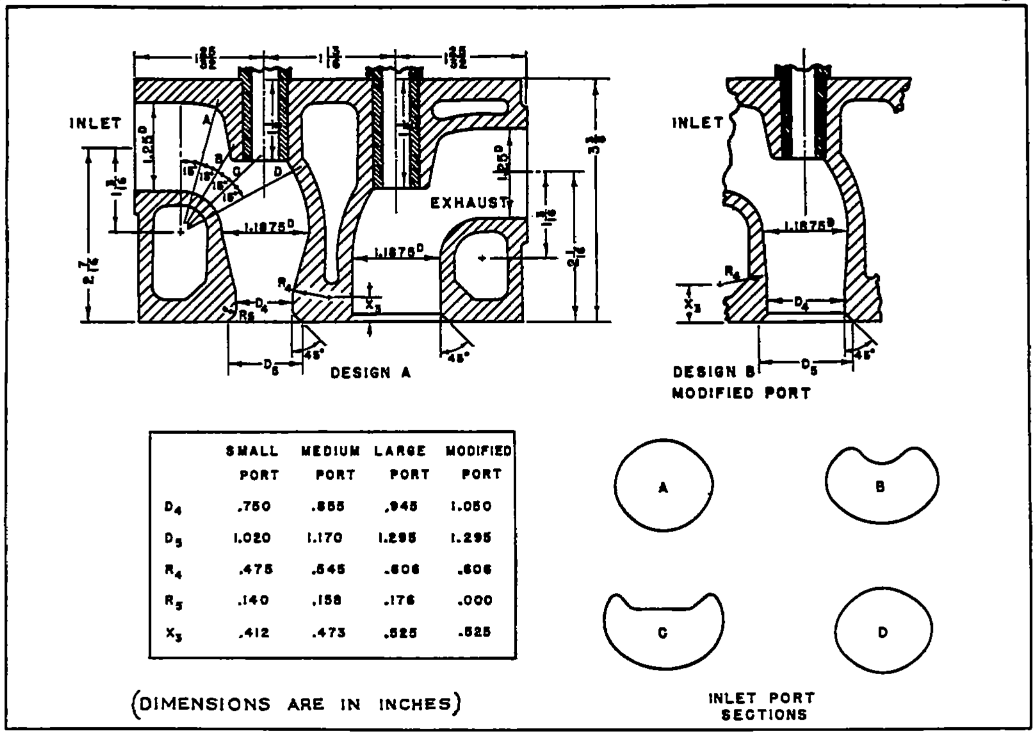

	SMALL PORT	MEDIUM PORT	LARGE PORT	MODIFIED PORT
D_4	.750	.855	.945	1.050
D_5	1.020	1.170	1.295	1.295
R_4	.475	.545	.606	.606
R_5	.140	.158	.176	.000
X_3	.412	.473	.525	.525

(DIMENSIONS ARE IN INCHES)

FIGURE 3.— PORT DESIGNS AND SIZES.

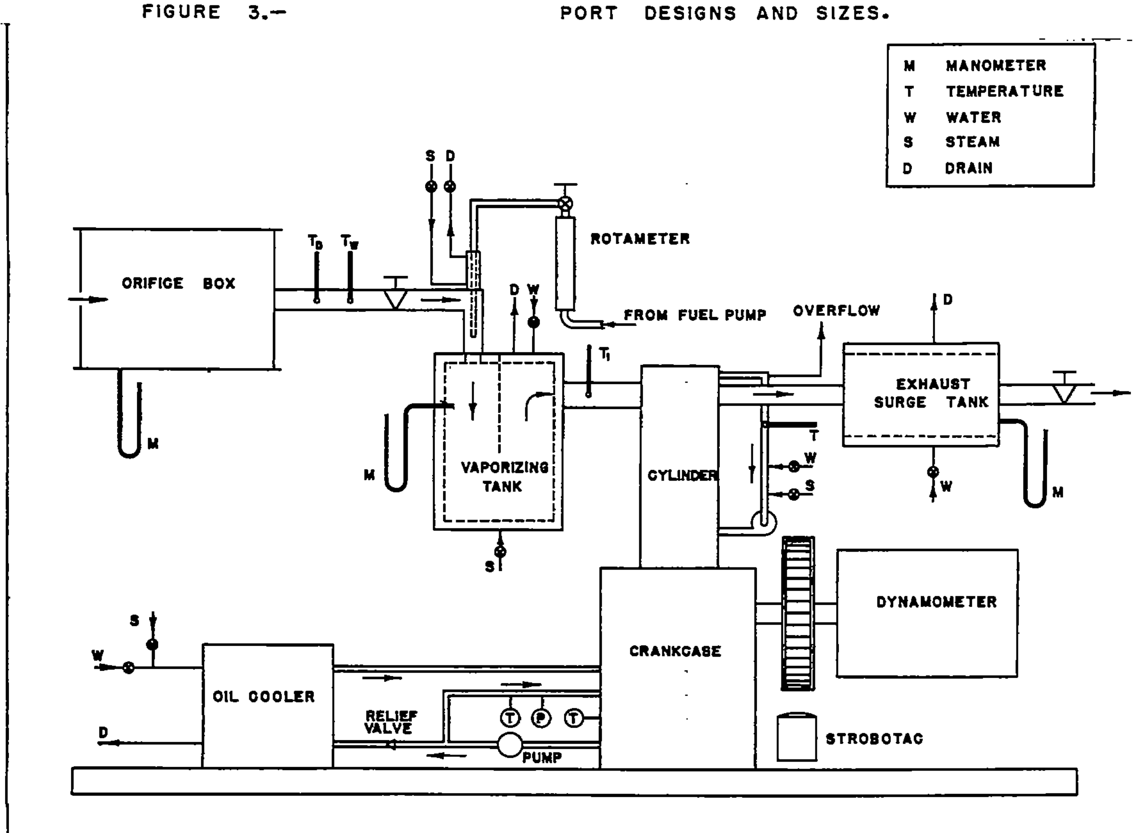

FIGURE 4.— SCHEMATIC LAYOUT OF THE ENGINE SETUP.

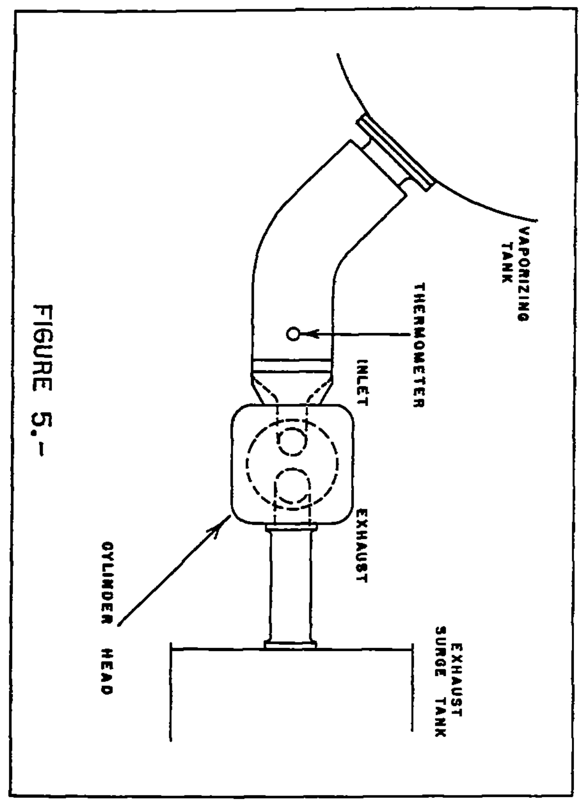

FIGURE 5.- SCHEMATIC LAYOUT SHOWING THE INLET AND EXHAUST ARRANGEMENT.

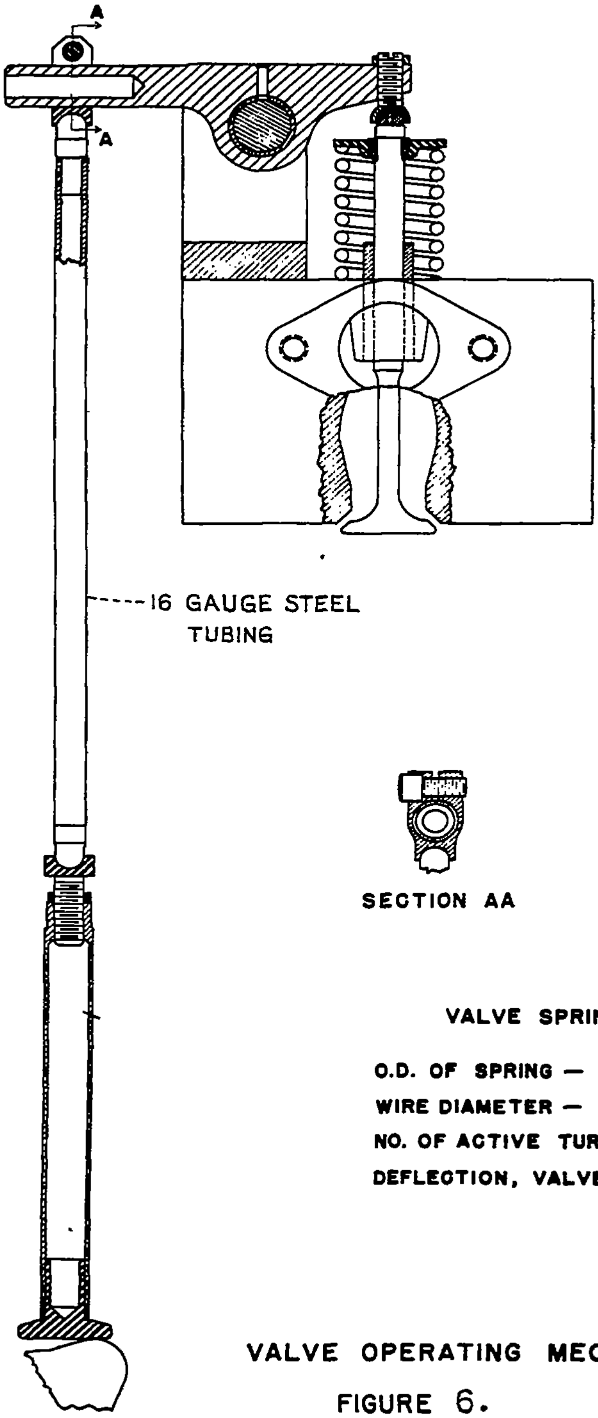

VALVE SPRING DATA

O.D. OF SPRING —	$1\frac{3}{8}$"
WIRE DIAMETER —	$\frac{3}{16}$"
NO. OF ACTIVE TURNS —	$4\frac{1}{2}$
DEFLECTION, VALVE CLOSED —	.153"

VALVE OPERATING MECHANISM.

FIGURE 6.

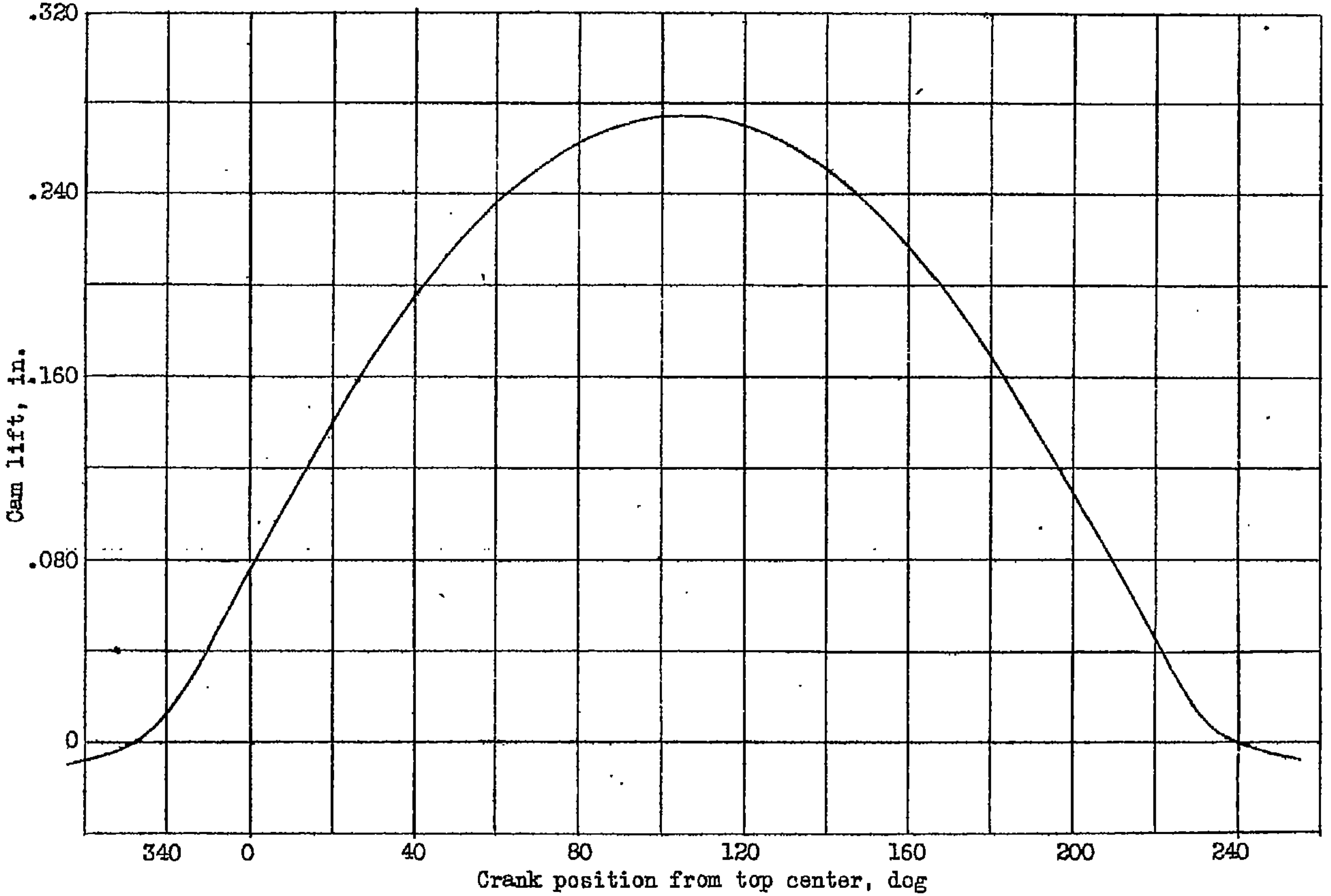

Figure 7.- Cam profile for inlet valve.

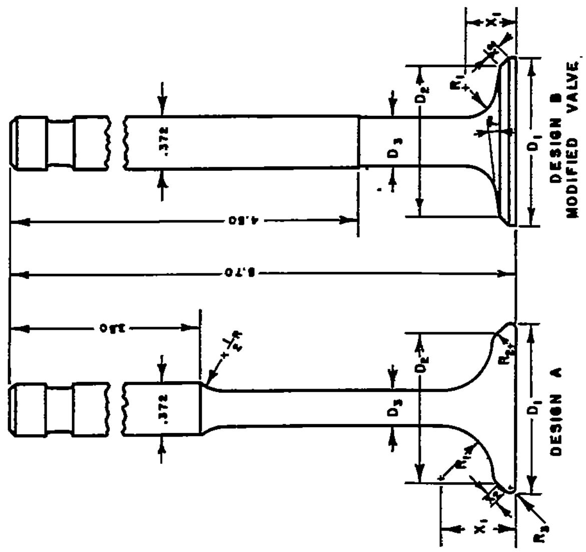

	SMALL VALVE	MEDIUM VALVE	LARGE VALVE	MODIFIED VALVE
D_1	.935	1.070	1.190	1.190
D_2	.830	.950	1.050	1.050
D_3	.199	.228	.253	.360
R_1	.284	.325	.362	.211
R_2	.126	.146	.162	.000
R_3	.028	.032	.036	.000
X_1	.413	.473	.525	.349
X_2	.068	.078	.087	.087

(DIMENSIONS ARE IN INCHES)

FIGURE 8.- VALVE DESIGNS AND SIZES.

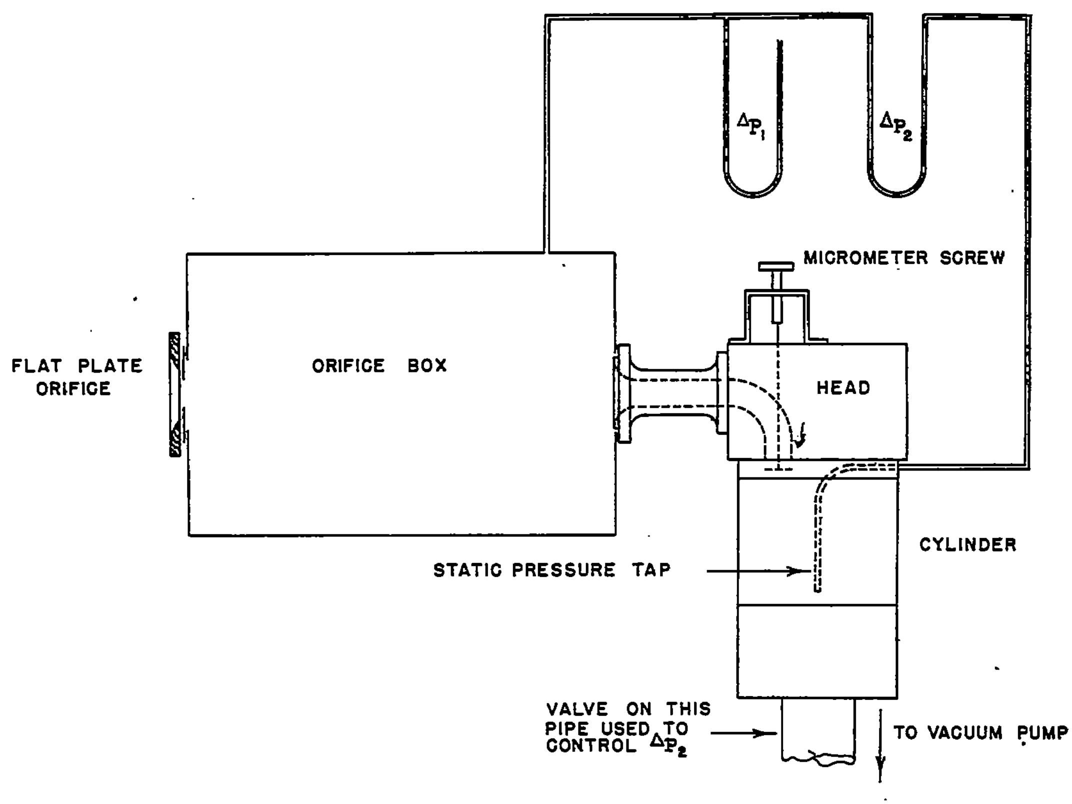

FIGURE 10.- SCHEMATIC LAYOUT OF THE STEADY-FLOW TEST APPARATUS.

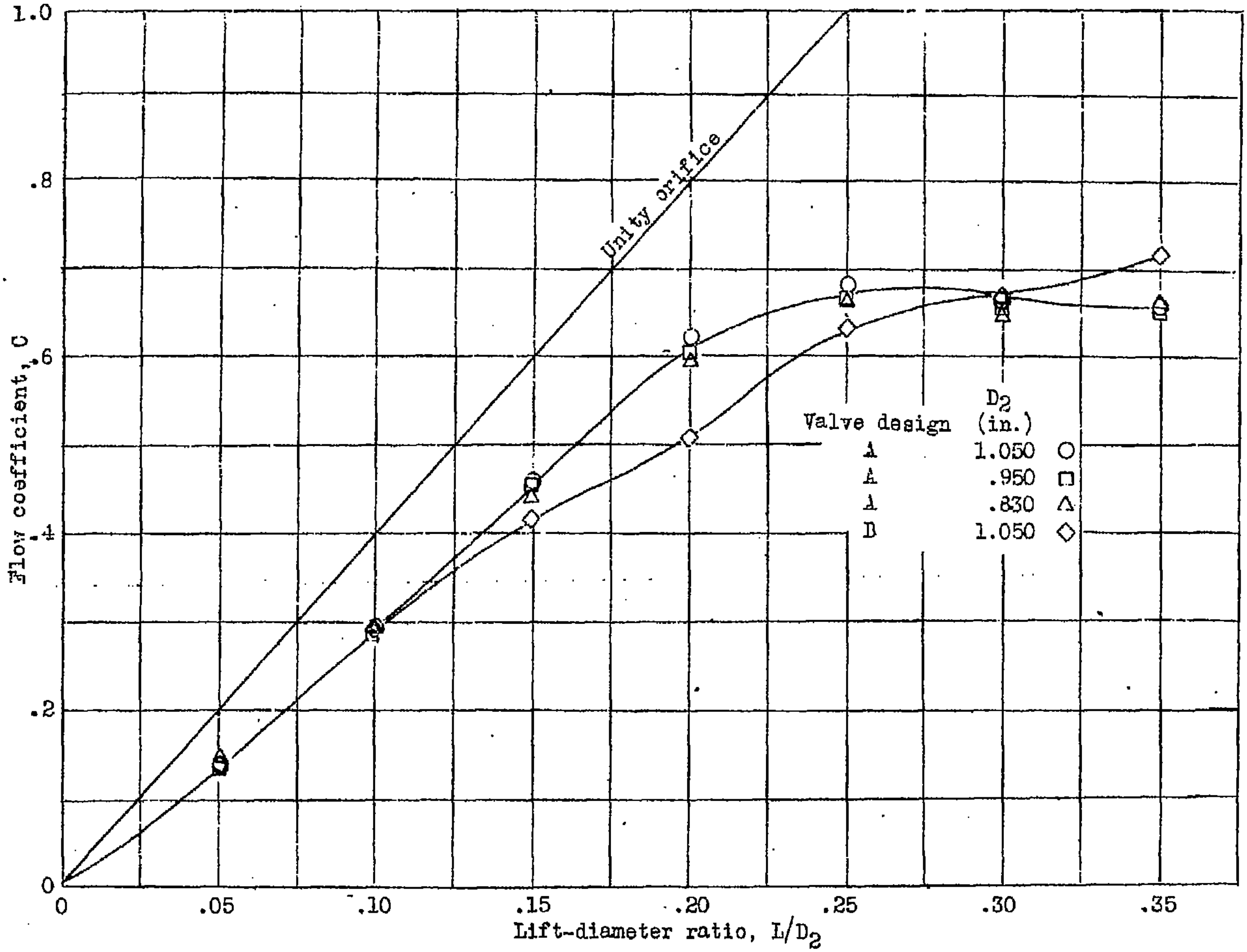

Figure 9.- Variation of flow coefficient with lift-diameter ratio.

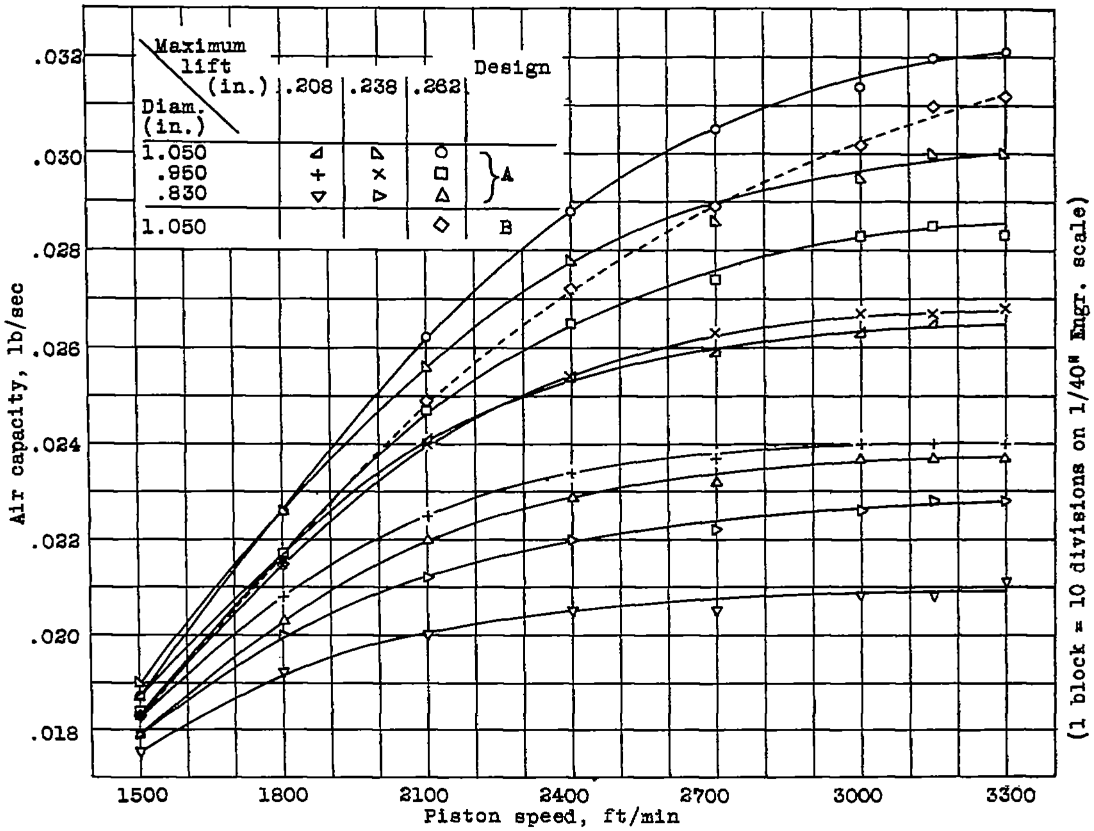

Figure 11.- Effect of inlet-valve design, diameter, and lift on air capacity.

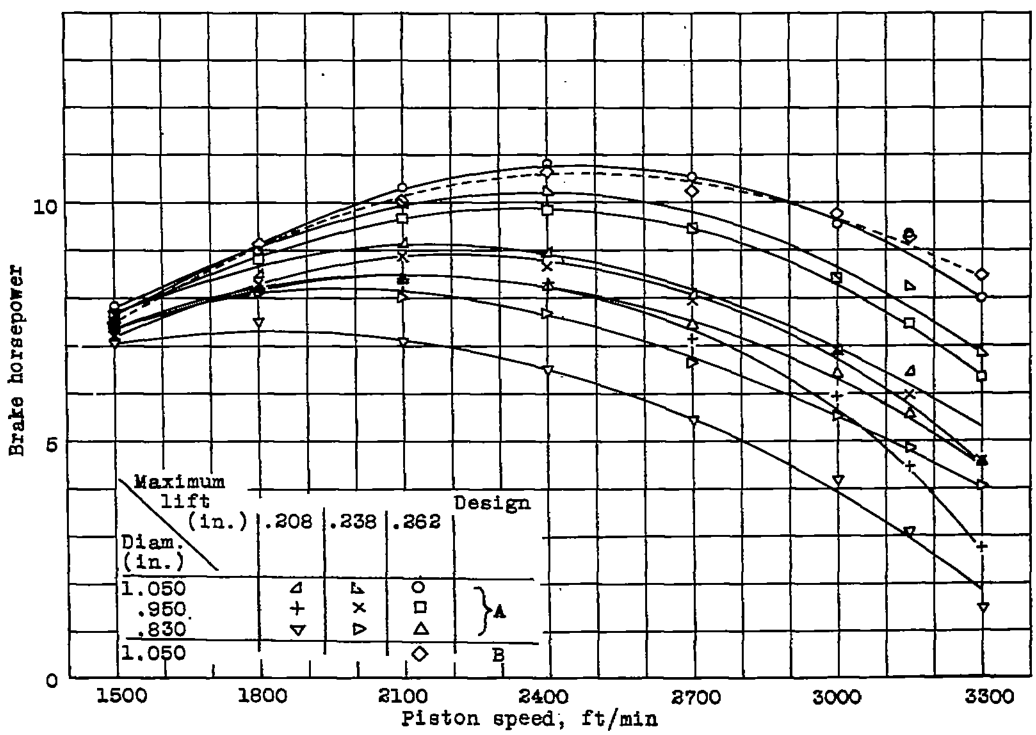

Figure 12.- Effect of inlet-valve design, diameter, and lift on power output.

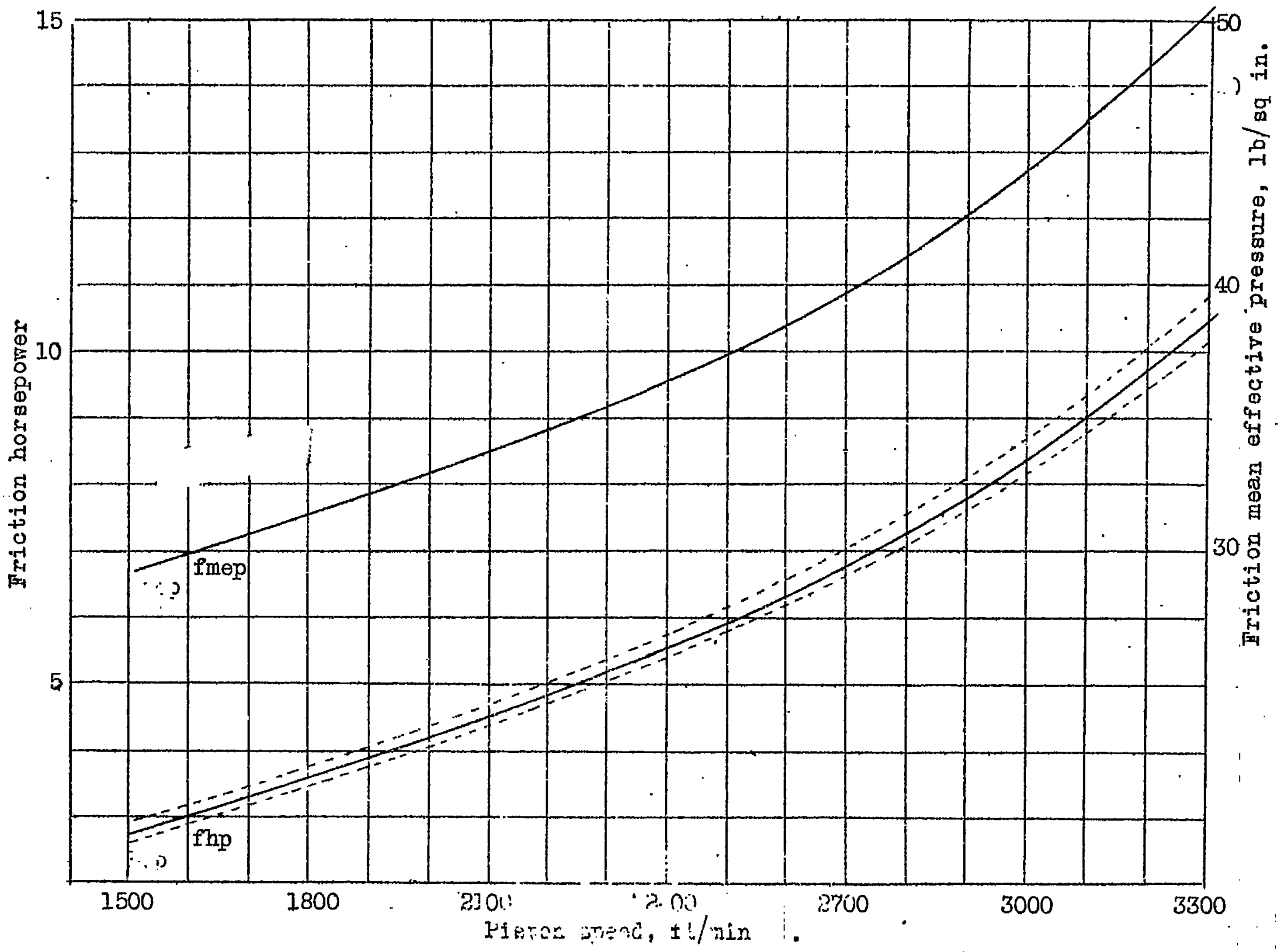

Figure 13.- Motoring friction for all valves and lifts, broken lines indicate the maximum deviation from the mean friction horsepower.

Diam. (in.) \ Maximum lift (in.)	.208	.238	.262	Design
1.050	◿	◺	○	A
.950	+	×	□	A
.830	▽	▷	△	A
1.050			◇	B

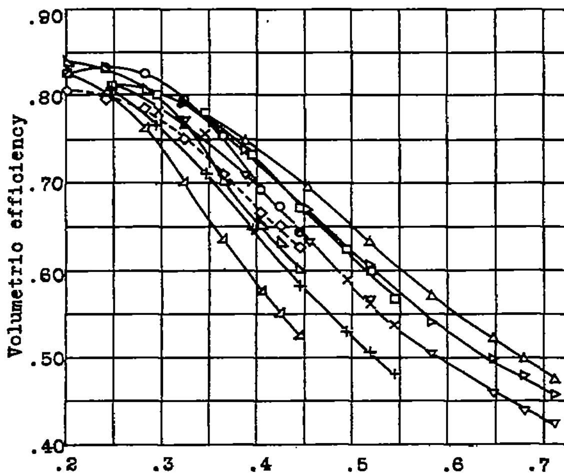

Figure 14

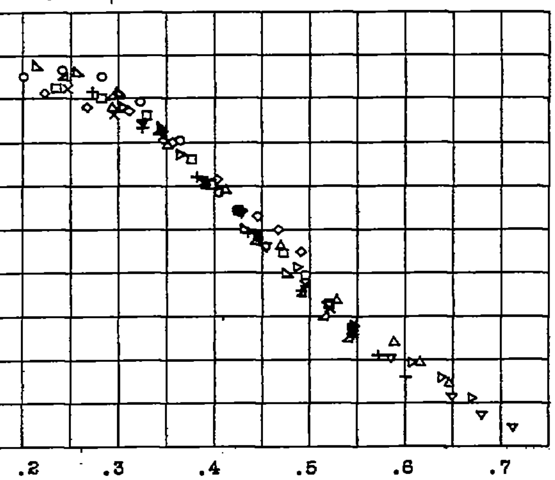

Figure 15

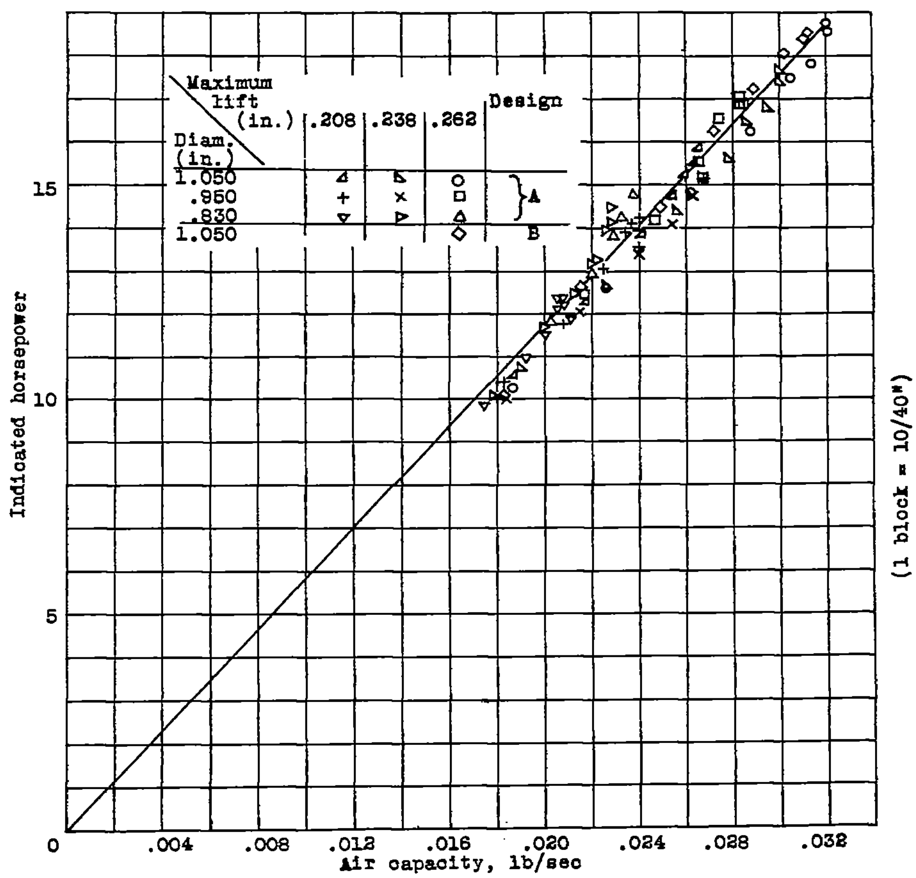

Figure 16.- Effect of air capacity on indicated horsepower.

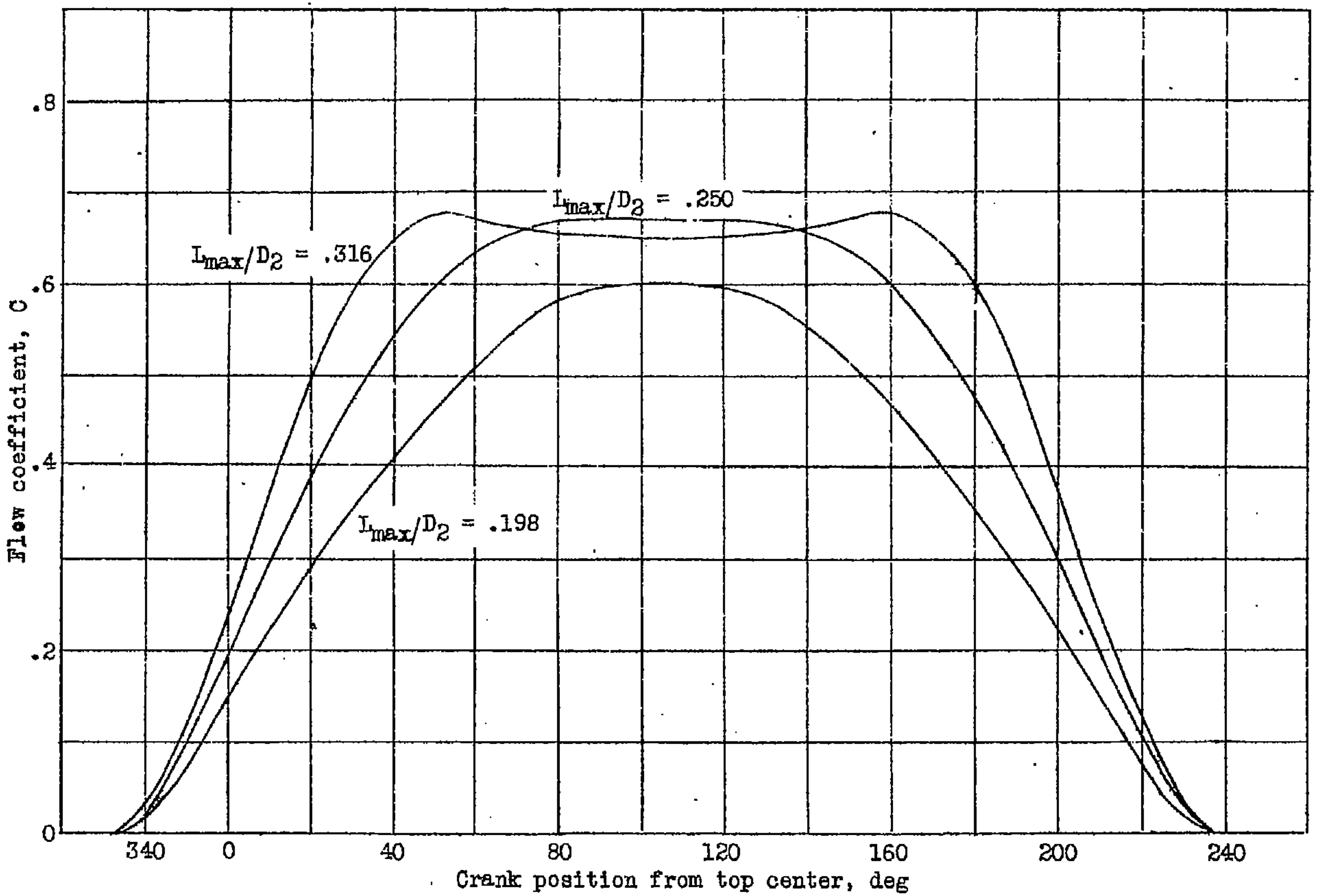

Figure 17.- Typical curves of flow coefficient against crank angle for valves of design A.

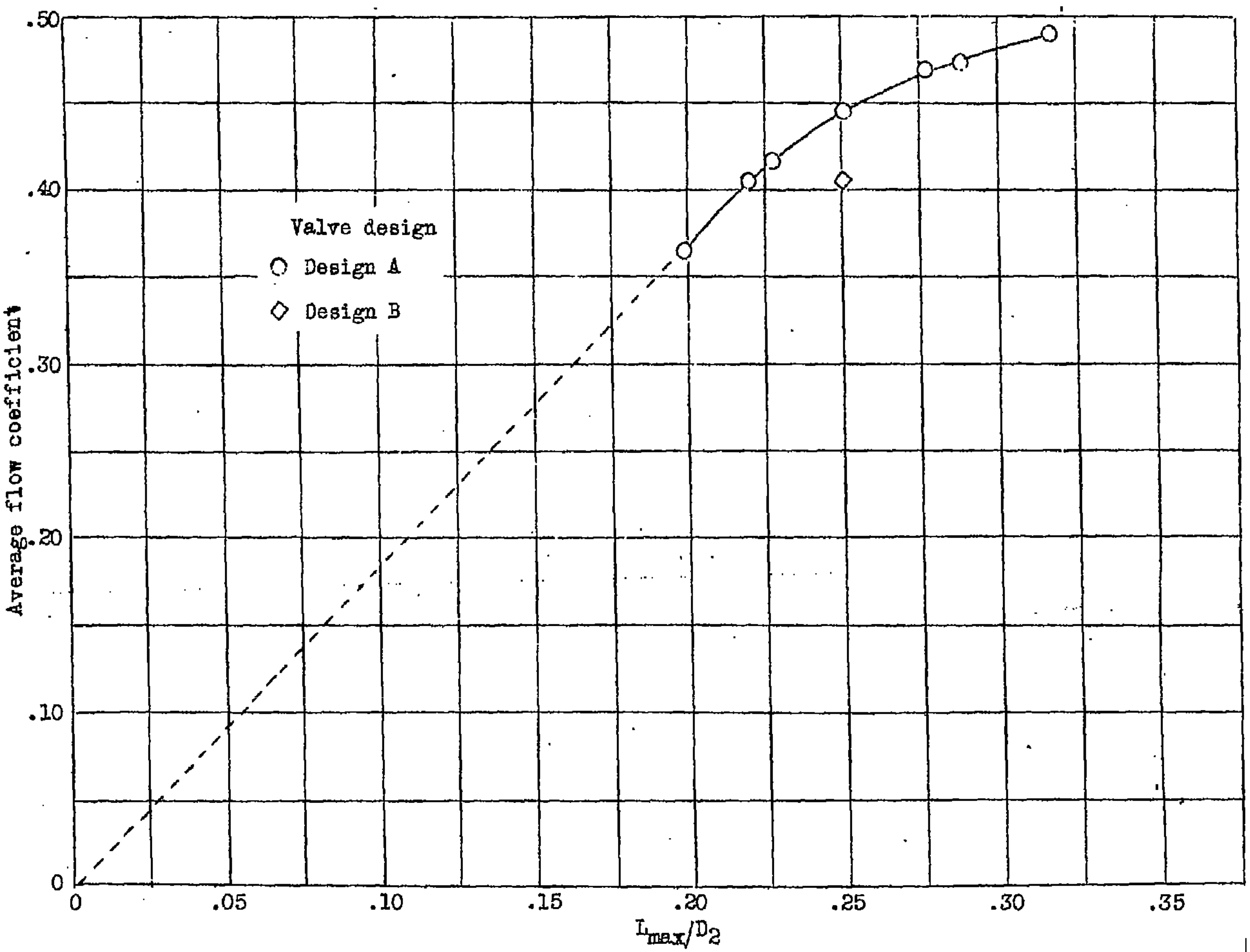

Figure 18.- Variation of average flow coefficient with L_{max}/D_2.